Early Pleistocene Human Humeri From the Gran Dolina-TD6 Site (Sierra de Atapuerca, Spain)

José María Bermúdez de Castro,[1]* José Miguel Carretero,[2,3] Rebeca García-González,[2] Laura Rodríguez-García,[2] María Martinón-Torres,[1] Jordi Rosell,[4] Ruth Blasco,[4] Laura Martín-Francés,[1,3] Mario Modesto,[1] and Eudald Carbonell[4,5,6]

[1]*Program of Paleobiología de Homínidos, Centro Nacional de Investigación Sobre Evolución Humana (CENIEH), Burgos,*
Paseo de la Sierra de Atapuerca s/n, 09002 Burgos, Spain
[2]*Departamento Ciencias Históricas y Geografía, Universidad de Burgos,*
Laboratorio de Evolución Humana, Edificio I+D+i, Plaza de Misael Bañuelos s/n, 09001 Burgos, Spain
[3]*Instituto de Salud Carlos III, Calle Sinesio Delgado 8, 28029 Madrid, Spain*
[4]*Institut Català de Paleoecologia Humana i Evolució Social, C/Escorxador s/n, 43003 Tarragona, Spain*
[5]*Area de Prehistoria, Universitat Rovira i Virgili (URV), Avinguda de Catalunya 35, 43002 Tarragona, Spain*
[6]*Visiting Professor Institute of Vertebrate Paleontology and Paleoanthropology of Beijing (IVPP), 142 Xizhimenwai Str., Beijing, China*

KEY WORDS human evolution; postcranial remains; taxonomy; phylogeny

ABSTRACT In this report, we present a morphometric comparative study of two Early Pleistocene humeri recovered from the TD6 level of the Gran Dolina cave site in Sierra de Atapuerca, northern Spain. ATD6-121 belongs to a child between 4 and 6 years old, whereas ATD6-148 corresponds to an adult. ATD6-148 exhibits the typical pattern of the genus *Homo,* but it also shows a large olecranon fossa and very thin medial and lateral pillars (also present in ATD6-121), sharing these features with European Middle Pleistocene hominins, Neandertals, and the Bodo Middle Pleistocene humerus. The morphology of the distal epiphysis, together with a few dental traits, suggests a phylogenetic relationship between the TD6 hominins and the Neandertal lineage. Given the older geochronological age of these hominins (ca. 900 ka), which is far from the age estimated by palaeogenetic studies for the population divergence of modern humans and Neandertals (ca. 400 ka), we suggest that this suite of derived "Neandertal" features appeared early in the evolution of the genus *Homo*. Thus, these features are not "Neandertal" apomorphies but traits which appeared in an ancestral and polymorphic population during the Early Pleistocene. Am J Phys Anthropol 147:604–617, 2012.

Humeri represent a substantial part of the postcranial hominin fossil record, and there is abundant literature dealing with the evolution of humeral morphology in hominins (e.g., Basabe, 1966; Senut, 1981; Pfeiffer and Zehr, 1996; Carretero et al., 1997; Larson et al., 2007). In particular, distal humeral morphology has received special attention, due to both its generally excellent preservation and the taxonomic and phylogenetic information it provides (Senut, 1981; Arsuaga and Bermúdez de Castro, 1984; Lague and Jungers, 1996; Carretero et al., 1999, 2009; Bacon, 2000; Yokley and Churchill, 2006).

The aim of this report is to present a descriptive and comparative study of two Early Pleistocene humeri recovered during the 2003–2007 field seasons from the TD6 level of the Gran Dolina cave site in Sierra de Atapuerca, northern Spain. This is the first opportunity to observe the morphology and biomechanical properties of the humerus of European Early Pleistocene hominins. Interestingly, the two specimens, ATD6-121 (immature) and ATD6-148 (adult) have relatively good preservation of the distal epiphysis, and thus we have the opportunity to test previous hypotheses concerning the taxonomic value of this part of the humerus in the genus *Homo* (Arsuaga and Bermúdez de Castro, 1984; Carretero et al., 1999, 2009; Yokley and Churchill, 2006). Some phylogenetic questions as well as possible evolutionary implications of these specimens are also briefly discussed.

MATERIALS AND METHODS

The Gran Dolina (TD) cave is placed in the southwestern slope of the Sierra de Atapuerca (Burgos, northern Spain). The cave is completely filled by interior and exterior facies deposits, which are up to 18 m thick. The TD infilling was exposed as the result of the construction of

Additional Supporting Information may be found in the online version of this article.

Grant sponsor: Dirección General de Investigación of the Spanish Ministerio de Educación y Ciencia (MEC); Grant numbers: CGL2009-12703-C03-01, 02, 03. Grant sponsor: Junta de Castilla y León; Grant numbers: BU005A09, GR249. Grant sponsors: Consejería de Cultura y Turismo of the Junta de Castilla y León; Fundación Atapuerca.

*Correspondence to: José María Bermúdez de Castro, Centro Nacional de Investigación Sobre Evolución Humana (CENIEH), Burgos, Paseo de la Sierra de Atapuerca s/n, 09002 Burgos, Spain. E-mail: josemaria.bermudezdecastro@cenieh.es

Received 16 May 2011; accepted 21 December 2011

DOI 10.1002/ajpa.22020
Published online 10 February 2012 in Wiley Online Library (wileyonlinelibrary.com).

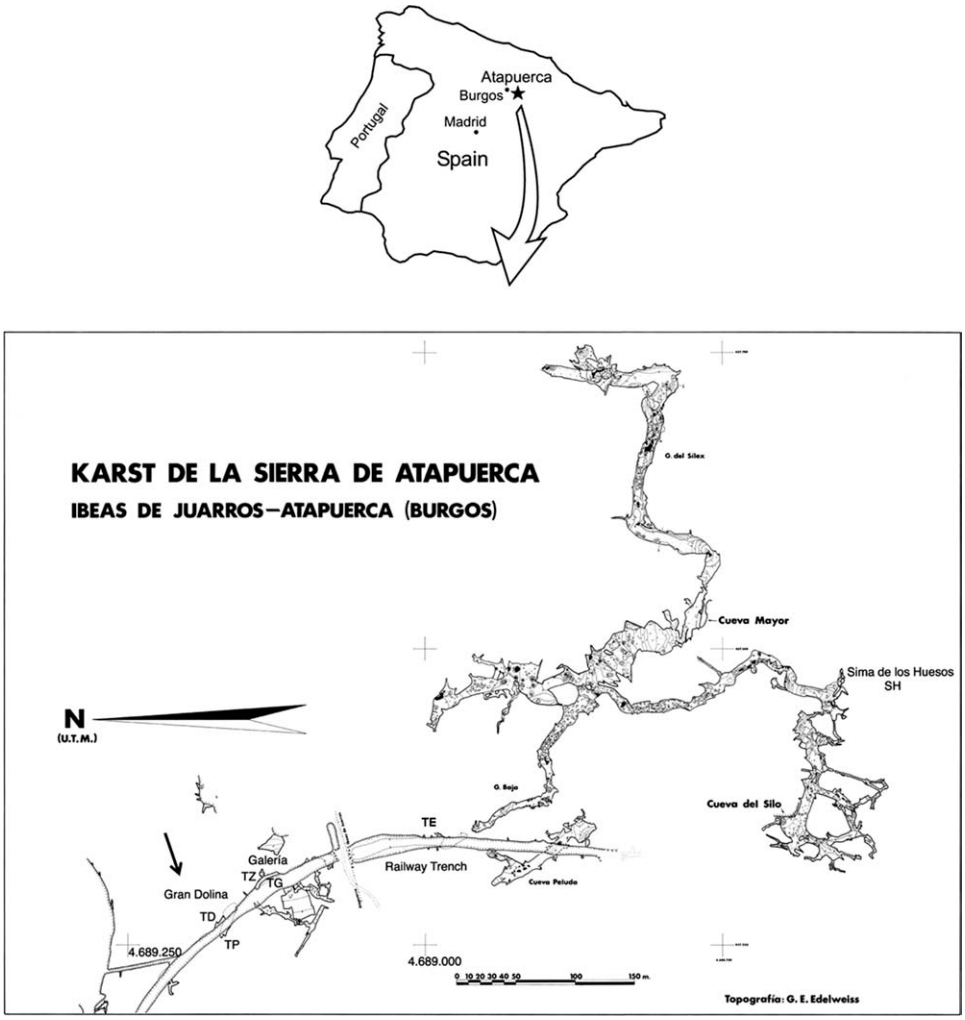

Fig. 1. Location of the Gran Dolina site (arrow) in relation to other sites in the Railway Trench at Sierra de Atapuerca (Burgos, Spain).

a railway trench at the end of the nineteenth century by a British mining company (Fig. 1). The history of the archeological investigations in TD can be found in Carbonell et al. (1999), and a detailed description of the lithostratigraphy of the site is in Parés and Pérez-González (1999).

The human humeri described in this report come from the TD6 level, where a collection of about 150 human fossil remains has been recovered so far (Carbonell et al., 1995; Bermúdez de Castro et al., 1997; Cabonell et al., 2005; Bermúdez de Castro et al., 2008). Figure 2a presents a detailed stratigraphy of the top sequence of the TD6 level (TD6-1 and TD6-2 Units), showing the place where the two human humeri were found. A plan of the position of these specimens in relation to other finds is in Figure 2b.

The arvicolids suggest that TD6 can be referred to the Biharian biochron (Cuenca-Bescós et al., 1999). The macromammal assemblage (near one thousand fossil remains) is biochronologically consistent with the end of the Early Pleistocene or early Cromerian (García and Arsuaga, 1999; van der Made, 1999). Paleomagnetic dating places TD6 in the Matuyama reversed Chron, hence older than 780,000 years (780 ka) (Parés and Pérez-González, 1995, 1999). These paleomagnetic data, combined with ESR and U-series, give an age range of between 780 and 857 ka for TD6 (Falguères et al., 1999). Thermoluminiscence (TL) ages (Berger et al., 2008) one meter below the Brunhes-Matuyama boundary (780 ka) give an age of 960 ± 120 ka for TD6. Because this age is consistent with the biostratigraphic and paleomagnetic evidence, Berger et al. (2008) proposed a likely chronological interval of 900–950 ka for the TD6 hominins. This age window corresponds to Marine Isotope Stage (MIS) 25, a relatively warm and humid interglaciation (Berger et al., 2008). Pollen analysis also suggests that the Aurora stratigraphic set (see Fig. 2a) was deposited under wet, temperate conditions (García-Antón, 1995).

The comparative samples employed in this study comprise adult and subadult recent and fossil specimens (Appendix Table A1, Supporting Information). The subadult specimen from Gran Dolina ATD6-121 was compared to five modern human collections chosen to cover a wide variability. Four subadult samples are composed of known age at death individuals (Hamman Todd, Spitafields, Lisboa, and Coimbra) and one of unknown age at death specimens (San Pablo). Given that dental calcification is better correlated with skeletal development than dental eruption, the age at death of immature

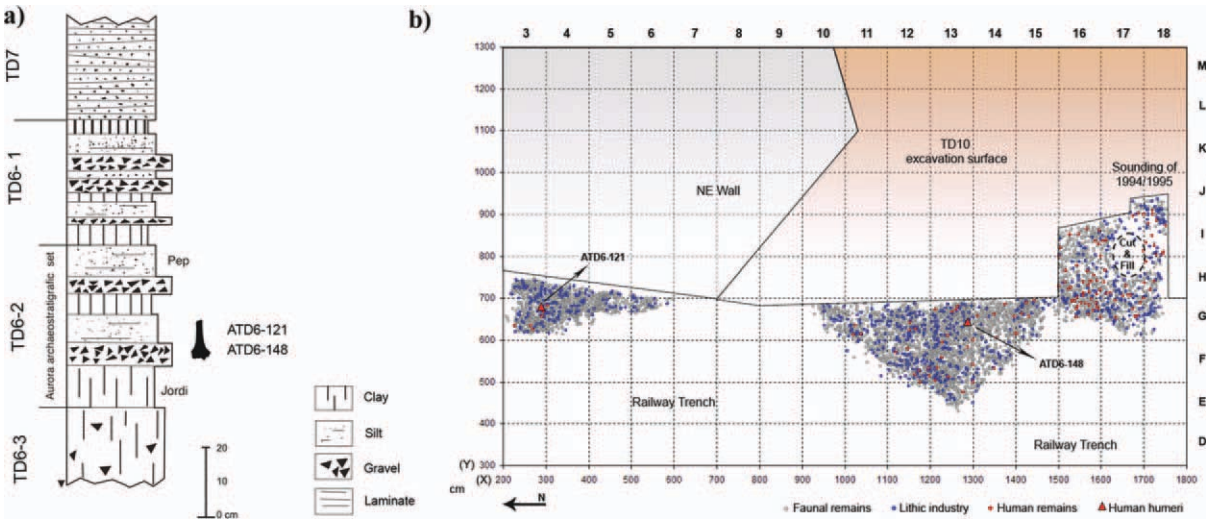

Fig. 2. (**a**) Top sequence of the lithostratigraphic unit TD6 from the Gran Dolina cave infilling (Matuyama Chron), which includes the "Aurora archeostratigraphic set" (AAS). This sequence corresponds to the middle area of the Gran Dolina section, and the observations were made at the level of squares G14 and G15 (see text for additional information). (**b**) Schematic plan of the TD6-2 level from south (squares D18 to M18) to north (squares D3 to M3), showing the situation (horizontal distribution) of the elements recovered in different field seasons. The test pit (south area) was excavated in 1994–95, whereas the excavations of the middle and north areas were excavated in 2003–10. The red triangles correspond to the human humeri.

individuals of our San Pablo sample was assessed based on dental calcification and root formation (tooth mineralization).

The mineralization stages of each tooth class were observed by conventional radiography and scored using the method of Moorrees et al. (1963a). The mean age of attainment of the different mineralization stages was interpolated from the European-American immature dental sample of Anderson et al. (1976). For individuals under 3 years of age we followed the method of Moorrees et al., (1963b).

In addition to the contemporary samples, we also include original data from the subadult Roc de Marsal 1, La Ferrassie 4 bis, La Ferrasie 3, and Le Moustier 2 and the data from Dederiyeh 1 (Kondo and Dodo, 2002).

The majority of the measurements from the modern samples were taken by the authors on the originals. All statistical analyses were performed with STATISTICA v 6.0 (StatSoft, Inc.).

All of the variables recorded for the TD6 humeri are defined in Appendix A (Supporting Information). Cross-sectional parameters of the adult specimen ATD6-148 were measured at the level of the 35% of total length (see Fig. 3).

RESULTS

The Adult Specimen ATD6-148

ATD6-148 represents the distal third of a left adult humerus (Fig. 3). By direct anatomical comparison with complete recent human humeri, we assessed that ATD6-148 represents approximately the segment between the 40 and 45% level proximally (mid–distal shaft, around where minimum perimeter is usually located) and the most distal articular point (0%) (distal at 0% following Trinkaus et al., 1994). The maximum preserved length of ATD6-148 is ~135 mm. However, it is important to note that the medial border, which is generally more prominent than the lateral one, is missing, so the actual length may be underestimated.

A nutrient foramen is on the medial surface, near the medial border, 100 mm from the most distal point of the specimen. The diameters, perimeter and cross-section were analyzed at 35% level, where the shaft is complete. Shaft perimeter is 57 mm. Given the absence of significant muscular markings at this point, we can assume that the shaft perimeter will vary little along the shaft (Trinkaus and Churchill, 1999) and that this value is probably very similar to the real minimum shaft perimeter (MSP). The cross-sectional shape at this level of MSP is subtriangular (Fig. 3).

Numerous cutmarks are present on the anterolateral, anteromedial, and posterior surfaces of the humerus, probably produced during the cannibalism process described for the TD6 assemblage (Fernández-Jalvo et al., 1996, 1999; Carbonell et al., 2010). Two possible percussion marks are also present near the edges of the fracture. The edges are smooth or slightly jagged, suggesting that the fracture was probably produced on green bone (see Villa and Mahieu, 1991).

The distal epiphysis is considerably damaged. In particular, the lateral epicondyle and the most extreme part of the medial epicondyle are missing. Both epicondyles are the origin of insertion of several extensor and flexor muscles of the forearm, wrist, and hand, which were probably removed during the cannibalism process, resulting in the breakage of these areas. The trochlea is better preserved, although the medial border is also damaged. The capitulum is missing. The olecranon fossa and the medial and lateral pillars adjacent to the fossa are well preserved. The olecranon fossa shows a subquadrangular shape and exhibits a natural and broad perforation, 8 mm wide. Therefore, although incomplete, it is possible to record directly some metrical variables in the distal epiphysis, as well as to estimate other variables.

Estimation of biepicondylar breadth (BB) and distal articular breadth (DAB). Given the importance of the biepicondylar breadth and the distal articular breadth for comparative purposes, we employed two

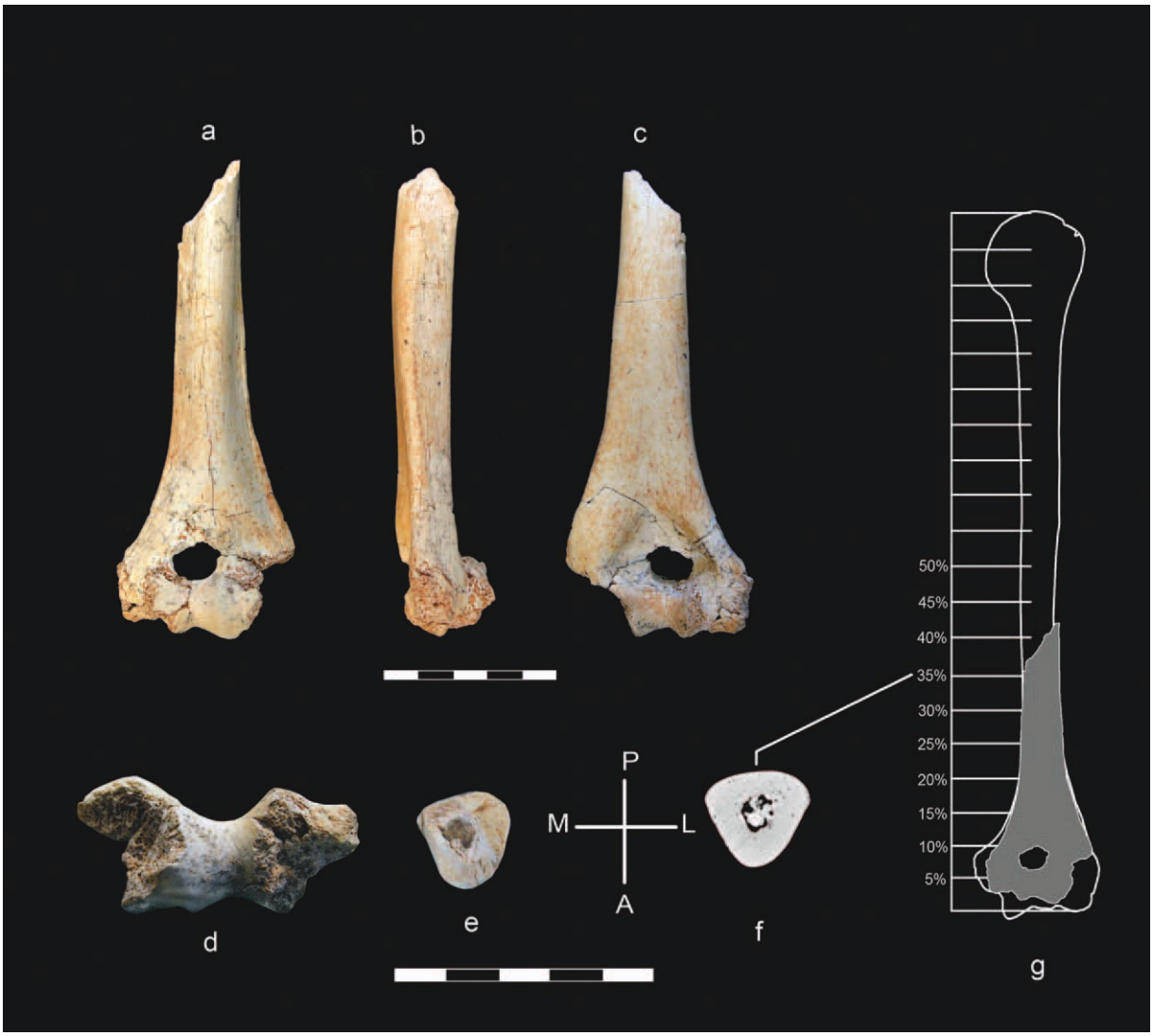

Fig. 3. ATD6-148 humerus from the TD6 level of the Gran Dolina cave site. (**a**) anterior view; (**b**) medial view; (**c**) posterior view; (**d**) distal view; (**e**) proximal view; (**f**) cross-section at 35% location; (**g**) sketch of the rough position of ATD6-148 in a silhouette of a complete humerus divided in percentages of length from distal to proximal following Trinkaus et al. (1994). [Color figure can be viewed in the online issue, which is available at wileyonlinelibrary.com.].

approaches to estimate these dimensions. The first approach was based on CT-scan images and 3D models to virtually reconstruct ATD6-148. For that purpose we employ as reference the Humerus XV from the Atapuerca-Sima de los Huesos (SH) site, since it has very similar shaft diameters, perimeter at the 35% level, olecranon fossa breadth, trochlear breadth, and lateral and medial pillar thicknesses. Humerus XV was rescaled and by superimposing both specimens, a BB of 60.4 mm and a DAB of 43.0 mm were obtained.

The second approach was mathematical. Olecranon Fossa Breadth (OFB) can be used in ATD6-148 to estimate BB and DAB. Nevertheless, in our recent modern human samples, OFB has a low correlation with these two variables. Furthermore, different relative proportions of OFB and BB have been demonstrated for several human species (Carretero et al., 1997, 2009). To prevent distortions in the estimations, we have preferred to not use OFB, and equations derived from modern humans, to estimate BB in human fossil humeri. Carretero et al., (2009) computed linear regression equations of biepicondylar breadth (BB) on minimum shaft perimeter (MSP) using two chronologically different recent human samples. However, we acknowledge that humeral shaft dimensions are to some degree developmentally and environmentally plastic (for example laterality due to handedness), so they may not be the best dimensions to estimate distal epiphyseal size (Trinkaus et al., 1994; Pearson, 1999; Auerbach and Ruff, 2006). In this study, BB and DAB were estimated from trochlear breadth (TRB), which can be measured directly in the specimen. We have developed regression equations of BB on TRB derived from different recent human samples and one from a pooled sample of all our modern human individuals (see Appendix Tables A2, A3, Supporting Information for details).

Given the robusticity of Pleistocene populations (e.g., Ruff et al., 1993, 1994; Pearson, 1999; Ruff, 2008, 2009), we have explored regression equations of BB on TRB derived from a pooled sample of Neandertals and

TABLE 1. Predicted biepicondylar breadth (BB) of ATD6–148 derived from linear regression formulae in appendix Table A3

Regression number	Regression from	BB on TRB		DAB on TRB	
		Predicted BB	95% CI	Predicted DAB	95% CI
1, 8	San Pablo	60.5	59.9–61.2	43.5	43.1–43.9
2, 9	Hamann–Todd	62.4	61.4–63.4	46.2	45.4–46.9
3, 10	Lisboa	59.8	58.2–61.5	43.5	42.6–44.3
4, 11	Pooled *Homo sapiens* sample	60.8	60.2–63.4	44.2	43.8–44.6
	Mean of recent samples	60.9 ± 1.1		44.4 ± 1.3	
5, 12	Sima de los Huesos	61.2	60.4–62.0	44.9	43.2–46.7
6, 13	Neandertals	61.7	60.0–63.4	44.8	43.7–45.9
7, 14	Neandertals + SH	61.8	60.6–62.9	44.9	44.1–45.8
	Mean of fossil samples	61.6 ± 0.3		44.9 ± 0.1	
	Total mean	61.2 ± 0.9		44.6 ± 0.9	

ATD6–148 minimum shaft perimeter (MSP) = 57.0 mm. ATD6–148 trochlear breadth (TRB) = 26.7 mm. CI = confidence interval for the mean BB at the given MSP or for the mean BB at a given TRB, or for the mean DAB at the given TRB. Number of valid cases for each sample and regression line as in Table A3.

TABLE 2. Comparisons of some linear dimensions of distal humerus in several fossil and recent specimens and samples

	BB	MPT	LPT	OFB
KNM-WT 15000F	55.0[a]	11.8	17.3	21.0
Gombore IB—7594	68.7	11.6	15.6	28.0
ATD6–148	**(61.2)**	**7.0**	**14.0**	**30.6**
BOD-VP-1/2[b]	60–66	9.0	18.0	31.0
Kabwe	62.0	11.9	18.4	26.1
Skhul IV	65.4	14.2	18.6	30.4
Omo Kibish I-r (KHS-1–30)	–	11.5	19.9	28.5
Omo Kibish I-l (KHS-1–31)	62.6	12.0	20.6	30.0
Cro-Magnon 1	63.4	14.0	20.7	27.4
Dolní Věstonice Individuals[c]	62.1 ± 2.4 (3)	9.1 ± 2.8 (4)	16.8 ± 1.7 (4)	27.6 ± 2.7 (4)
Sima de los Huesos	60.0 ± 4.8 (8)	8.6 ± 1.3 (9)	15.7 ± 2.0 (6)	29.4 ± 1.7 (9)
Neandertals	63.2 ± 3.7 (17)	7.7 ± 1.8 (23)	15.6 ± 2.2 (21)	29.4 ± 2.2 (21)
Sepúlveda pooled sex (N = 30)[b]	67.3 ± 3.3	12.7 ± 1.7	18.1 ± 1.6	25.9 ± 2.4
Aranda de Duero males (N = 71)[b]	60.3 ± 4.1	12.2 ± 1.9	17.7 ± 2.3	23.8 ± 2.4
San José Cemetery pooled sex (N = 45)[b]	59.3 ± 5.2	11.1 ± 1.8	16.6 ± 1.9	24.4 ± 2.3
San Pablo Monastery (N = 96)	59.1 ± 4.6	11.0 ± 2.3	17.2 ± 2.0	24.4 ± 2.5
Lisboa (N = 87)	53.8 ± 5.5	9.7 ± 2.0	14.9 ± 2.1	23.1 ± 2.5
Hamann–Todd (N = 62)	61.8 ± 5.8	11.2 ± 2.2	18.3 ± 2.5	25.3 ± 3.0

BB = biepicondylar breadth; MPT = medial pillar thickness; LPT = lateral pillar thickness; OFB = olecranon fossa breadth[a] Estimated value from Walker and Leakey (1993).
[b] Data from Carretero et al., 2009.
[c] Sample composed by the humeri of DV 13 (r,l), DV 14 (r,l), DV 15 (r,l), and DV 16 (r,l). None of DV16 humeri preserve BB. Raw data from Sládek et al., 2000. Variable means calculated by the authors.

Atapuerca-SH specimens. Appendix Table A3 (Supporting Information) shows the different regression equations employed in this analysis.

As we see in Table 1, the estimates of BB based in TRB derived from modern human and fossil samples are very similar, suggesting that articular dimensions may not be very plastic (Trinkaus et al., 1994). In this aspect, the average of the estimates of BB based on TRB derived from modern samples is 60.9 mm, and the average derived from fossil samples is 61.6 mm. The average of all estimates is 61.2 mm (Table 1). In our view, 61.2 mm is a reasonable value for the BB of ATD6-148. Regarding DAB, estimates based on modern humans and fossil samples are also quite similar, so we have taken the mean of all estimates (44.6 mm) as the value for DAB in ATD6-148. This value is also close to the one obtained through the 3D morphological approach.

Finally, it is not possible to make reliable sex estimation. While the MSP of the TD6 humerus fits better with the values obtained for females in several modern samples of known sex, TRB, BB and DAB are closer to the majority of male mean values. Therefore, we prefer to consider the sex of this individual as undetermined.

Comparative analysis. The distal humeri of *H. heidelbergensis* (Atapuerca-SH) and Neandertals (*H. neanderthalensis*) are characterized by a relatively wide and deep olecranon fossa and thin lateral and overall medial pillar adjacent to the fossa (Carretero et al., 1997; Yokley and Churchill, 2006). Recently, Carretero et al. (2009) have also described these features in the African Middle Pleistocene specimen from Bodo (Middle Awash, Ethiopia). In ATD6-148, it is possible to measure directly the maximum breadth of the olecranon fossa (OFB): 30.6 mm (Table 2). With this value, the OFB of ATD6-148 is also relatively wide when compared to the BB (Table 3). Most noticeable is the high OFB/BB index of ATD6-148 in comparison to those of contemporary modern humans, the Cro-Magnon and Gombore IB-7594. The value of the index in the TD6 humerus is similar to those of the Atapuerca-SH sample and the estimated value for the Bodo specimen (Table 3).

TABLE 3. Comparisons of some relative dimensions of the distal humerus in several fossil and recent specimens and samples

	Pillar index	MPT/OFB	MPT/BB	LPT/BB	OFB/BB
KNM-WT 15000F	68.2	56.2	21.4[a]	31.4[a]	38.2[a]
Gombore IB—7594	74.3	41.4	16.9	22.7	42.7
ATD6–148	50.0	22.9	11.4	22.8	50.0
BOD-VP-1/2[b]	50.0	29.0	13.6–15.0	27.3–30.0	47.0–51.7
Kabwe	64.7	45.6	19.2	29.7	42.1
Skul IV	78.5	46.7	21.6	28.3	46.5
Omo Kibish I (r+l)	58.2	40.0	19.1	32.9	47.9
Cro Magnon 1	67.6	51.1	22.1	32.6	43.2
Dolní Věstonice Individuals[c]	53.8 ± 12.4 (4)	34.0 ± 13.4 (4)	13.0 ± 3.2 (3)	25.8 ± 1.5 (3)	46.6 ± 1.1 (3)
Sima de los Huesos	54.9 ± 10 (6)	29.0 ± 3.8 (8)	14.0 ± 1.7 (7)	25.8 ± 1.9 (6)	48.7 ± 3.7 (8)
Neandertal sample	51.0 ± 10.0 (20)	26.9 ± 5.5 (21)	12.0 ± 2.5 (14)	25.4 ± 2.2 (13)	46.1 ± 2.7 (16)
Sepúlveda (N = 30)[b]	70.8 ± 10.6	50.1 ± 9.4	20.0 ± 2.6	28.3 ± 2.1	40.8 ± 3.6
Aranda males (N = 71)[b]	69.4 ± 9.7	47.4 ± 8.7	20.3 ± 3.4	29.5 ± 4.4	39.7 ± 5.7
San José (N = 45)[b]	67.1 ± 9.6	–	18.7 ± 2.1	28.0 ± 2.6	41.2 ± 3.4
San Pablo (N = 107)	63.4 ± 9.9	45.3 ± 11.1	18.5 ± 2.9	29.1 ± 2.6	41.4 ± 3.9
Lisboa (N = 88)	65.1 ± 11.5	42.4 ± 9.5	17.9 ± 2.8	27.8 ± 2.9	43.1 ± 4.3
Hamann Todd (N = 63)	61.4 ± 9.6	44.6 ± 8.9	18.0 ± 2.5	29.7 ± 2.5	41.2 ± 3.8

All indices multiplied by 100. Number in parentheses indicates sample sizes.[a] Estimated values.
[b] Data from Carretero et al., 2009.
[c] Sample composed by the humeri of DV 13 (r,l), DV 14 (r,l), DV 15 (r,l), and DV 16 (r,l). None of DV16 humeri preserve BB. Raw data from Sládek et al., 2000. Indices calculated by the authors.

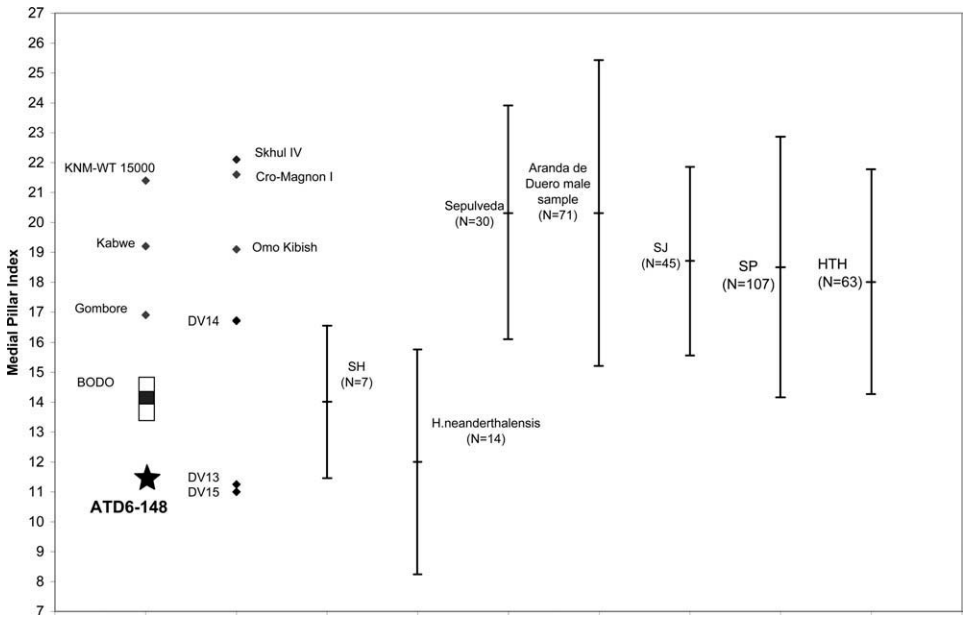

Fig. 4. Medial pillar index (medial pillar thickness/biepicondylar breadth) × 100 calculated for the fossil humeri, two human fossil samples, and five recent human samples (modified from Carretero et al., 2009). Neandertal sample as in Carretero et al. (1997; Table 18, p 400). SH, Sima de los Huesos; SJ, San José; SP, San Pablo; HTH, Hamann–Todd; DV, Dolní Věstonice. Numbers in parentheses indicate sample sizes. Vertical bars for recent human samples represent 1.5 standard deviations around the sample mean. Vertical bar for Bodo indicates the range of the pillar index calculated for this specimen. Black star indicates ATD6-148 position.

Although KNM-WT 15000 is an immature individual, his humeral developmental state is close to the final morphology and proportions. The humeri of this specimen show a narrow OFB and thick medial and lateral pillars, as it is the rule in recent *H. sapiens*. On the other hand, the Kabwe humerus has no clear stratigraphic provenance and it could well be Middle Pleistocene or Holocene in age (Trinkaus, 2009). Nevertheless Yokley and Churchill (2006) have observed that the Kabwe E-898 humerus is morphologically more similar to modern humans than to Neandertals and concluded that the "archaic" African elbow morphology shows a range of variation that overlaps that of both Neandertals and modern humans. Despite the chronological doubts, we prefer to include this fossil in Tables 2 and 3 and in Figure 4 for informative purposes, although it will not be mentioned hereafter in the discussion.

In association with this feature, the lateral and medial pillars are of ATD6-148 are particularly thin. The thickness of the medial pillar is 7.0 mm, whereas the thickness of the lateral pillar is 14.0 mm (Table 2). These values yield a low pillar index, similar to the one obtained for the

TABLE 4. Cortical thickness of the humeral cross-section at 35% of bone total length

	Total area (mm^2) [TA]	Cortical area (mm^2) [CA]	Percent cortical area [(CA/TA) × 100]
ATD6–148	232.7	203.4	90.0%
Bodo (BOD-VP-1/2)[a]	263.47	212.57	80.7%
Sima de los Huesos (N = 5)[a]	318.82 ± 35.98	254.96 ± 45.43	79.5% ± 8.0%
Neandertals (N = 10)[b]	300.16 ± 52.72	240.70 ± 45.43	80.0% ± 5.0%
Euroamerican (N = 38)[b]	279.20	181.6 ± 7.0	65.0%
Amerindians Georgia Coast (N = 37)[b]	271.90	182.0 ± 8.0	66.9%
Amerindian California (N = 71)[b]	258.80	189.6 ± 5.3	73.3%
Jomon Japanese (N = 25)[b]	271.40	167.40 ± 8.7	61.7%
Tennis players (N = 45)[b]	437.90	365.80 ± 10.6	83.5%
Early Upper Palaeolithic[c]	269.5 ± 36.1	200.9 ± 33.5	74.3% ± 4.8%
Late Upper Palaeolithic[c]	261.8 ± 36.9	189.6 ± 28.6	72.6% ± 8.2%

[a] Data from Carretero et al., 2009.
[b] Data from Trinkaus et al. (1994). TA for these samples was computed by the authors as the cortical area plus medullary area given in Table 4 of Trinkaus et al. (1994).
[c] Data from Churchill (1994).

TABLE 5. Comparison of cross-sectional parameters of ATD6–148 with other left fossil humeri

	Sex	BB	I_x	I_y	I_{max}	I_{min}	J	Relative J ($J/BB^4 \times 1000$)
ATD6–148	M	(61.2)	4484.0	4249.2	4527.5	4205.7	8733.2	0.60
BOD-VP-1/2	M	60–66	6001.6	4882.6	6003.9	4880.3	10884.2	0.84 – 0.57
SH Humerus XV	M	61.1	6060.2	4867.1	6615.2	4312.0	10927.3	0.78
SH Humerus III	M	66	8055.6	8365.8	8871.3	7550.1	16926.9	0.89
Shanidar 6	F	56			3328.8	2162.7	5491.5	0.56
Tabun 1	F	55.8	3981.5	2810.3	4032.2	2760.2	6792.4	0.77
Kebara 2	M	60.4	9086.2	7186.0	9397.3	6874.8	16272.1	1.20
Shanidar 1	M	64.5	7761.1	6584.8	8765.1	5580.7	14345.8	0.80
Saint-Césaire	M		5144	4076	5386	3832	9218	
Skhul II	F		2609	2336	3769	2176	5945	
Skhul VII	F		2314	1778	2349	1743	4093	
Skhul IV	M	65	5692	4712	5799	4605	10404	0.58
Skhul V	M	65	5076	6072	6073	5075	11148	0.62
Early upper palaeolithic		62.4 ± 4.8 (8)	6312.8 ± 1723.1	4911.2 ± 1337.2			11223.9 ± 2999.9	0.74 ± 0.2
Late upper palaeolithic		59.5 ± 4.1 (10)	5585.66 ± 1483.9	4797.9 ± 1643.2			10383.6 ± 3014.0	0.83 ± 0.2
Modern human sample		58.3 ± 4.7 (40)	5681.6 ± 2185.9	4664.2 ± 2129.6	4332.2 ± 2258.7	5721.5 ± 2782.5	10345.8 ± 4243.8	0.89 ± 0.2

I_x and I_y = second moments of area about x and y axes (mm^4). I_{max} and I_{min} = maximum and minimum second moments of area (mm^4). J = polar second moment of area (mm^4). Data of Bodo and SH humeri from Carretero et al. (2009). Data of Shanidar, Tabun, Kebara, and Skhul specimens from Trinkaus and Churchill (1999). Data of Saint-Césaire from Trinkaus et al. (1999). Data of early and late upper Paleolithic from Churchill (1994). Data of modern humans by the authors from Medieval specimens of San Pablo Monastery, Burgos, Spain.

Bodo specimen (Carretero et al., 2009) and the Neandertal sample, and slightly lower than that of Atapuerca-SH sample (Table 3). Concerning the index that relates the medial pillar thickness and the BB, ATD6-148 is close to the average of the Neandertal sample and not far from the average of the Atapuerca-SH sample and the Bodo specimen (Table 3). As we can see in Figure 4, the placement of the ATD6-148 specimen is remarkable with regard to other Pleistocene specimens, like KNM-WT 15000F, Gombore IB-7594, Omo Kibish I, or Cro-Magnon 1. ATD6-148 is in the range of variation of Atapuerca-SH, Neandertal, and Bodo specimens. We must note here that among the Middle Upper Paleolithic humeri from Dolní Věstonice, Shang, and Trinkaus (2010) report a variable relatively medial pillar thickness compared with OFB, with two specimens, DV-13 and DV-15, showing particularly low indices that fall well within Neandertal values. Also these authors report a relatively thin medial pillar relative to OFB in the Early Upper Paleolithic left humerus from Tianyuan 1 (see also Shang et al, 2007). When MPT and OFB are compared to BB it is also clear that Dolní Věstonice humeri display the same condition found in Neandertals and SH hominids, contrary to the Cro-Magnon specimen (Table 3, Fig. 4), thus strengthening the frequencial nature of this trait in our species.

As mentioned above regarding the cross-sectional parameters, with the same total section area, ATD6-148 shares with Neandertals and the Atapuerca-SH hominins a thicker cortical bone (Table 4). The Gran Dolina fossil is, in this aspect, thicker than the Neandertal male from Spy and similar to those from La Ferrassie 1 and Saint Césaire 1. The relative CA reflects the bone resistance to axial compression and tension (Trinkaus et al., 1994, 1999; Trinkaus and Churchill, 1999). When we standardized it by BB^2, CA of ATD6-148 (5.42%) is coincident with the mean found in our modern human sample (5.45% ± 0.73%, N = 43).

For the rest of mechanical parameters (Table 5), all of Middle and Late Pleistocene specimens, Neandertals and Atapuerca-SH and the Early and Upper Palaeolithic

Fig. 5. ATD6-121 subadult humerus from the TD6 level of the Gran Dolina cave site. (**a**) Anterior view; (**b**) posterior view; (**c**) medial view. [Color figure can be viewed in the online issue, which is available at wileyonlinelibrary.com.].

samples (data from Churchill, 1994), are well within the 95% equiprobability ellipse of recent humans. I_{max}/I_{min} in our fossil sample indicates a cross-section shape that is rounder than in most recent specimens.

Finally, the absolute value of polar moment of inertia (J) for ATD6-148 falls again inside our modern human sample range of variation (Table 5). However, when we standardized it by the biepicondylar breadth to the fourth power (our indicator of size), this value is somewhat lower in comparison to the mean of modern humans, meaning that the biepicondylar breadth of ATD6-148 is larger than those of modern humans with the same J. The same situation happens with some (but not all) the Neandertal specimens such as La Chapelle aux Saints, La Ferrassie 1, Spy 2, and Krapina 160, and with Cro-Magnon and Barma Grande 2 from the Upper Palaeolithic (Churchill, 1994).

The child specimen ATD6-121

This specimen consists of the entire diaphysis (up to the surgical neck proximally) and the distal epiphysis of the right humerus of a subadult individual (Fig. 5). In spite of its fragility, ATD6-121 is admirably preserved. The most significant relief of the shaft is the intertubercular sulcus, which reaches a maximum width of 12 mm. A nutrient foramen is present on the medial surface, 50 mm from the most distal point of the humerus. On the posterior aspect of the epiphysis, a wide and deep olecranon fossa is noticeable. The wall of the fossa is very thin.

Maximum length and age at death estimations. For comparative purposes, it is necessary to estimate the age at death of the individual ATD6-121. The maximum humeral intermetaphyseal length (IL) is the most useful variable to estimate age at death in modern subadult individuals (Maresh, 1970; Fazekas and Kosa, 1978; Scheuer et al., 1980; Scheuer and Black, 2000; Smith and Buschang, 2004). However, because these values are based on modern children, with modern diets and likely larger body sizes for the same age, this approach has likely limitations when applying it to fossil specimens. The total preserved length of ATD6-121 is 121.2 mm. Taking into consideration the shaft dimensions (diameters and perimeters) and anatomical landmarks, such as the muscular impressions, bicipital sulcus development, or the nutritional foramen position, a maximum length between 150 and 155 mm can be reasonably assumed for this humerus. Based on this "anatomically estimated" humeral intermetaphyseal length (150–155 mm), age at death of this specimen could be estimated based on modern standards. Nevertheless, the growth and developmental pattern, body proportions and expected body size are unknown in the ATD6 population. To partially overcome this problem, and to cover a wider variability, age at death for the ATD6-121 was estimated based on several modern samples with different body size and proportions. First, we derived a regression line from each of our five comparative samples, where the dependent variable was age at death and the independent variable was the humeral intermetaphyseal length. Given ATD6-121 size, we discard the possibility that it belonged to a child younger than 3 years old. Thus, we employed the regression formula E given by Cowgill (2010) for individuals ≥3 years old.

TABLE 6. Age prediction regression formulae by sample

Sample	Constant	Slope	R^2	SEE
Spitalfields[a] (n = 90)	−5.09	0.06	0.91	0.92
Portugueses[a] (n = 48)	−4.92	0.07	0.77	2.11
HTH[a] (n = 18)	−4.91	0.06	0.61	1.85
San Pablo[a] (n = 25)	−6.03	0.07	0.86	1.01
Dart[b] (n = 42)	−5.46	0.07	0.86	1.43
Kulubnarti[b] (n = 61)	−7.25	0.08	0.82	1.57
Mistihalj[b] (n = 29)	−10.50	0.09	0.88	1.55
Indian Knoll[b] (n = 72)	−8.74	0.09	0.92	1.34
California[b] (n = 70)	−7.94	0.08	0.93	1.25
Point Hope[b] (n = 61)	−7.64	0.08	0.89	1.31

Dependent variable is age and independent variable is intermetaphyseal humeral length.[a] Samples measured by the authors.
[b] Regression equations derived from Cowgill et al. (2010).

All of the regression equations employed in this study and the age at death obtained with each are shown in Table 6. We employed the two values of the intermetaphyseal length estimation (150–155 mm), so two ages at death and their respective standard error are obtained for each formula. To derive an estimate of the weighted mean and a likely age range for ATD6-121 based on average of the values obtained from each regression equation, a meta-analysis was carried out. In the meta-analysis, each of the ages derived from each regression equation is treated as an individual case, so the standard error of the estimation for each regression formulae is incorporated in the final calculation. In this way, a mean age is calculated within the 99% confidence limit. This analysis is similar to the one used by Roberts et al. (2008) to calculate the dental age of an individual based on different tooth stages.

To test the consistency of our estimations, we compared the age of three late Pleistocene individuals of known dental age with the age predicted with this

method (Table 7). Estimated age is close to the real dental age of LagarVelho 1 and Qafzeh 10. Even in the case of the large humerus of Dederiyeh 1, the dental age is within the 99% confidence interval.

With a humeral intermetaphyseal length of 150 mm for ATD6-121, our analysis provides an age of 4.6 years, with a 99% confidence interval between 3.5 and 6 years. With a humeral intermetaphyseal length of 155 mm, the age at death obtained is 4.0 years old, with a 99% confidence interval between 4 and 6 years. Therefore, it is reasonable to infer an age at death between 4 and 6 years old for ATD6-121.

We are aware that when age at death is estimated, it is important to consider the growth and developmental patterns of the species under study. Although we know that dental development pattern in this human species is similar to that of modern humans (Bermúdez de Castro et al., 2010), much less is known about postcranial growth and its relationship with dental development (García-González et al., 2009). Therefore, we should bear in mind that the conclusions derived from the metrical study of ATD6-121 rely on the age at death estimations.

TABLE 7. Dental ages and ages predicted from humeral intermetaphyseal length in several Late Pleistocene immature individuals

Specimen	HIL (mm)	Dental age (years)	Age estimated (years)	CI (99%)
Lagar Velho[a]	143	4.5	4.11	(3.03, 5.18)
Qafzeh 10[b]	168	6	6	(4.93, 7.08)
Dederiyeh 1[c]	125	1.5	2.66	(1.5, 3.74)

In all cases, dental age is between 99% confidence interval of age estimated. HIL: humeral intermetaphyseal length. Dental ages derived from Minugh Purvis (1988). Humeral intermetaphyseal length derived from a: Trinkaus et al. (2002) b: Tillier (1999) and c: Kondo and Dodo (2002).

Comparative analysis. Table 8 shows the main absolute and relative dimensions of ATD6-121 compared to a pooled sample (San Pablo and the Portuguese collections) of children 3–6 years old (the wider range for estimated age of ATD6-121). Figure 6 shows the variation of several indices in the modern samples and the relative position of some fossil specimens.

All humeral dimensions recorded in ATD6-121 fall within the range of variation of the 3- to 6-year-old group of the modern sample, except for the measures related to the olecranon fossa, medial pillar and width of the distal end.

Among Neandertals, distal metaphyseal breadth (DMB) is absolutely large in Roc de Marsal (Madre-Dupouy, 1992) and Dederiyeh 1 (Kondo et al., 2000) but not in the younger individual from Le Moustier 2 (Fig. 6). DMB of ATD6-121 falls within the range of variation of the modern sample (Table 8). Relative to MaxL, DMB decreases slightly with age in modern children, indicating a different growth rate in these two dimensions. In this regard, Le Moustier Neandertal specimen is close to the mean of modern children with the same age at death (0–1 years), but the index is higher in Dederiyeh 1 with 1.5 years (Fig. 6). Therefore, a relatively large humeral distal end does not characterize all immature Neandertals. This particular skeletal proportion seems to appear early in the development, but not from the very beginning. ATD6-121 shows a DMB proportion above the mean for the 3- to 6-years old group for modern children, but based only on this result it is difficult to be certain that the TD6 hominins share with Neandertals enlarged humeral distal epiphyseal proportions (Table 8; Fig. 6).

TABLE 8. Comparison of linear and relative dimensions of ATD6–121 and recent subadult humeri in the same age class

Sample	ATD6–121	Pooled sample		
		3–6 years old		
Age group	4–6 years old	*N*	Mean	Std. Dev.
Intermetaphyseal length (IL)	150–155	16	151.81	15.54
Midshaft A-P diameter	12.7	17	10.84	1.08
Midshaft M-L diameter	11.3	17	10.88	1.31
Midshaft perimeter	39	17	35.24	3.33
Minimum shaft perimeter	32	16	35.00	2.71
Distal metaphyseal breadth (DMB)	33	13	29.28	2.75
Olecranon fossa breadth (OFB)	17.1	15	15.90	1.35
Olecranon fossa depth	8.5	15	5.86	1.25
Coronoira fossa breadth	12.1	16	10.30	1.32
Radial fossa breadth	7.7	14	7.38	1.41
Medial pillar thickness (MPT)	3.6	16	6.21	0.80
Lateral pillar thickness (LPT)	9.1	15	9.29	1.36
Midshaft index	76.1	17	100.90	12.95
Robusticity index	25–26	16	23.21	2.32
Pillar index	39.6	15	68.26	11.95
Total Area (mm^2)	76.3			
Cortical Area (mm^2)	63.1			
% Cortical Area (CA/TA)	82.7%			
I_{max} (mm^4)	478.7			
I_{min} (mm^4)	438.4			
J (mm^4)	917.1			
MPT/DB	10.9	13	21.68	2.49
MPT/OFB	21.1	15	39.38	5.05
OFB/DMB	51.8	13	54.15	3.91
DMB/IL	22–21.3	13	19.87	1.87

All linear dimensions are in millimeters.

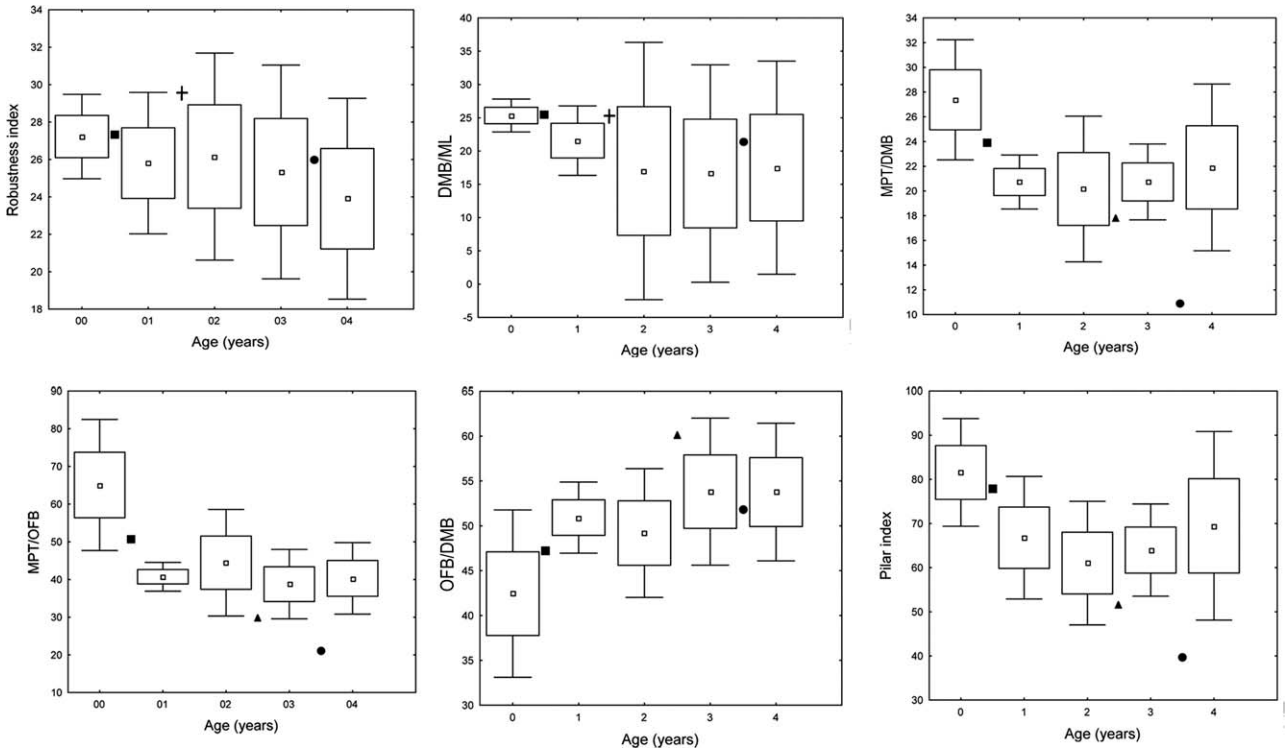

Fig. 6. Variation of different indices of the humerus in recent child samples of different ages and the position of some fossil specimens. Box and whisker plots represent the mean (white square) plus minus one (box) and two (whisker) standard deviations. Black Square = Le Moustier 2; Black Cross = Dederiyeh 1; Black Triangle = Roc de Marsal; Black Circle = ATD6-121.

It is interesting to note that the distal end of ATD6-121 seems to display the same morphological pattern than the adult specimen ATD6-148, which is also present in the adult Neandertals, the Atapuerca-SH hominins, and the Bodo specimen. This pattern includes a relatively wide and deep olecranon fossa and relatively thin lateral and medial pillars. This morphological pattern is also found in the Le Moustier 2, Roc de Marsal 1, and Dederiyeh 1 subadult Neandertals (Table 8; Fig. 6).

Finally, the presence of thick bone cortices is a well-known characteristic of all the representatives of the genus *Homo*, with the exception of later Holocene sedentary *H. sapiens*. While this characteristic is clearly present in adult specimens, it is also present at an early developmental age in the early and middle Pleistocene hominins from the Gran Dolina and SH sites in Sierra de Atapuerca (Carretero et al., 1997, 1999), as well as in very young Neandertal individuals such as Kiik-Koba (5–12 months; Vlcêk, 1973), Dederiyeh 1 (1.5 years; Akazawa et al., 1995; Dodo et al., 1998; Kondo et al., 2000), La Ferrassie 6 (3–5 years; Heim, 1982), and Cova Negra (Arsuaga et al., 2007).

ATD6-121 displays at a mid-distal shaft level (at 35% location) a percent cortical area (CA/TA) of 82.7%. This relative cortical thickness is above the values of Skhul I (67%) and Lagar Velho I (53%), slightly older than ATD6-121 but within its general age range, around 4–5 years (Trinkaus et al., 2002). ATD6-121 value is also above the mean of a recent juvenile sample from the Denver Growth Study sample (4–5 years, $N = 20$; %CA = 68%) reported by Trinkaus et al. (2002). These data confirm the early ontogenetic appearance of relatively thick bone cortices in the TD6 hominins. In Cowgill (2010), the bone cortical thicknesses and J values of immature Neandertals are always higher than the mean obtained in her modern sample and our fossil immature sample.

DISCUSSION

In this report, we present the descriptive and comparative study of two new important Early Pleistocene specimens recovered from the TD6 level of the Gran Dolina cave site in Sierra de Atapuerca. The distal epiphyses of ATD6-121 and ATD6-148 exhibit all of the traits that are characteristic of the genus *Homo*. However, these specimens display relatively thin lateral and medial pillars and a relatively wide olecranon fossa. In previous studies some authors have observed that Neandertals and European Middle Pleistocene hominins (represented by the Atapuerca-SH specimens) exhibit a relatively large and wide olecranon fossa and thin medial and lateral pillars (Arsuaga and Bermúdez de Castro, 1984; Carretero et al., 1997; Yokley and Churchill. 2006).

Regarding the evidence of these features in the hominin fossil record, most australopithecines show a shallow and narrow olecranon fossa, which is set almost in the middle of the biepicondylar width. As a consequence, the medial and lateral pillars are almost equivalent in width (Senut, 1981). The condition in early *Homo* (e.g., Gombore IB-7594) and *H. ergaster* (or African *H. erectus*, e.g., KNM-WT 15000F) is different, with a deeper olecranon fossa, which is more medially placed, and with the lateral pillar being thicker than the medial one. Nevertheless, the two pillars are thick, and the olecranon fossa is relatively narrow with respect to the biepicondylar breadth. The distal humeral epiphysis of Dmanisi hominins D2680 and D4507, dated to 1.8 Ma (Gabunia et al.,

2000; Lumley et al., 2002; Lordkipanidze et al. 2007), clearly display the same morphology that, in accordance with the Yokley and Churchill (2006) hypothesis, would be the primitive condition for the genus *Homo*. This ancestral condition seems to be more frequent in early and recent *H. sapiens* (e.g., Omo-Kibish 1, Skhul IV, Cro-Magnon 1) (Carretero et al., 1997), although among them we have also found, less frequently, the derived condition (e.g., Dolní Věstonice and Tianyuan; Shang and Trinkaus, 2010). In contrast, a relatively wide and deep olecranon fossa and the relatively thin lateral and medial pillars represent a distinctive pattern very frequent in the Middle and Late Pleistocene Neandertal lineage (Carretero et al., 1997) and, as we mentioned above, this pattern is also present in the Bodo partial distal humerus BOD-VP-1/2 (Carretero et al., 2009). Yokley and Churchill (2006) have confirmed that Neandertals clearly differentiate from other hominins in having a relatively large olecranon fossa and narrow distodorsal medial and lateral pillars. In spite of the fact that the proximal ulnar morphology of certain "archaic" African hominins, such as KNM-BK 66, Klasies River Mouth (Churchill et al., 1996; Groves, 1998; Pearson et al., 1998), and Border cave (Pearson and Grine, 1996) is morphologically more similar to Neandertals, there is a significant correlation between the olecranon fossa superior–inferior diameter and the olecranon process superoinferior length (Yokley and Churchill, 2006). For Yokley and Churchill (2006), the presence of a relatively large olecranon fossa and narrow distodorsal medial and lateral pillars is a derived condition in Neandertals. In contrast, a relatively narrow olecranon fossa and wide distodorsal medial and lateral pillars would be the primitive condition in hominins. Because Neandertals and modern humans share a common ancestor, the less frequent presence of the derived condition in "archaic" and recent modern humans may be, according to Yokley and Churchill (2006), the result of either gene flow, or a morphological convergence produced by similar behavioral practices.

Thus, it is clear that the TD6 humeri share with Neandertals some derived features in the distal epiphysis with regard to the primitive *Homo* pattern. The thickness of the lateral and medial pillars of ATD6-148 is even below the average of the Atapuerca-SH and Neandertal samples, whereas the OFB/BB index is higher than the average of these samples. Moreover, the thin lateral and medial pillars as well as a wide olecranon fossa are also observed in the infantile humerus ATD6-121. How can we interpret this variability in an European hominin population that is nearly one million years old and that, according to genetic data, predates by at least 200–400 ka the mean age obtained by several authors for the time of the most recent common ancestor of modern humans and Neandertals (Noonan et al., 2006; Krause et al., 2010, Endicott et al., 2010)?

In 1997, some of us proposed the name *H. antecessor* to accommodate the variability observed in the hypodigm of the TD6 hominins (Bermúdez de Castro et al., 1997). This species was characterized by a combination of primitive traits shared with early *Homo*, primitive traits retained by modern humans, and derived traits also shared with modern humans (Bermúdez de Castro et al., 1997, 1999; Arsuaga et al., 1999; Carretero et al., 1999; Lorenzo et al., 1999; Rosas and Bermúdez de Castro, 1999). Furthermore, it was hypothesized that *H. antecessor* could represent the last common ancestors to modern humans and Neandertals, mainly based on the presence in the TD6 hypodigm of some cranial and postcranial features shared with these two hominin lineages (Bermúdez de Castro et al. 1997; Arsuaga et al, 1999; Carretero et al., 1999; Lorenzo et al., 1999; García-González et al., 2009; Gómez Olivenza et al., 2010). However, the primitive pattern in the dentition of the TD6 hominins contrasted with the fully Neandertal pattern of the Atapuerca-SH hominins (Bermúdez de Castro, 1993; Martinón-Torres et al., 2012). Thus, the relationship between TD6 hominins and the Neandertal lineage was questioned, and some of us proposed a discontinuity between the European Early Pleistocene human populations, represented by the TD6 hominins, and the European Middle Pleistocene populations, represented by the Atapuerca-SH hominins (Bermúdez de Castro et al., 2003). Posterior studies of an enlarged hypodigm revealed that a few TD6 dental traits were derived with regard to Early Pleistocene African populations and shared with European Middle Pleistocene hominins, Neandertals, and other Eurasian Pleistocene populations (Martinón-Torres et al., 2006; Gómez-Robles et al., 2007). Furthermore, the study of a large dental sample from Pleistocene Eurasian and African sites revealed that the TD6 hominins shared a characteristic Eurasian pattern in the dentition with the European Middle and Early Upper Pleistocene hominins (the so-called Neandertal lineage) and other Pleistocene Asian groups (Martinón-Torres, 2006; Martinón-Torres et al., 2007). In addition, the study of the TD6 mandibles also demonstrates a close relationship between the TD6 hominins and other Eurasian populations (Carbonell et al., 2005; Bermúdez de Castro et al., 2008).

The number of features specifically shared between the TD6 hominins and the Neandertal lineage is small, and with the exception of the data presented here and the dental traits mentioned above, no other "Neandertal" traits have been identified in the TD6 hypodigm so far. In view of these shared traits, some researchers could suggest that the evolution of the Neandertal lineage in Europe might stretch back to nearly one million years ago. However, this hypothesis is difficult to sustain since it would imply that the divergence of modern humans and Neandertals occurred remarkably earlier than it is usually proposed by most of the palaeogenetic studies (ca. 400 ka vs. ca. 900 ka), (Noonan et al., 2006; Krause et al., 2010; Endicott et al., 2010). At this point, it is interesting to note that the lower range of the 95% confidence interval for *H. sapiens* and *H. neanderthalensis* time divergence obtained in some molecular studies is coincident with the geochronological ages obtained for the TD6 hominins (Ovchinnikov et al., 2002; Green et al., 2008) so the discrepancy between the fossil and the genetic data would not be that large. In addition, most of the genetic studies assume zero gene flow between both lineages, potentially making these estimates much younger.

However, we believe that the most parsimonious explanation for the expression of "Neandertal" features in the European Early Pleistocene fossils is that some of the so-called "Neandertal" features (including the ones recorded in the present study) are traits that appeared in an earlier and ancestral population and may be highly polymorphic. This situation would also explain the presence in the TD6 hominins of a suite of features typically considered characteristic of the Neandertal lineage, and it would still be compatible with a phylogenetic position

for *H. antecessor* close to the common ancestry of Neandertals and modern humans.

ACKNOWLEDGMENTS

The authors acknowledge all members of the Atapuerca Research Team for their dedication and effort. Lucía López-Polin, from the IPHES Restoration and Conservation Department, made the cleaning of the specimens, whereas Pilar Fernández Colón and Elena Lacasa Marquina, from the CENIEH Restoration and Conservation Department helped with the conservation, and manipulation of the specimens. The composition of the figures was prepared by Susana Sarmiento and Elena Santos. They are very grateful to the following people and institutions for providing access to the skeletal collections in their care: Eugenia Cunha and Ana Luisa Santos (Instituto de Antropologia de la Universidade de Coimbra), Alexandra Marçal (Museu Bocage, Museu Nacional de História Natural, Lisboa), Yohannes Haile-Selassie, Bruce Latimer and Lyman Jellema (Cleveland Natural History Museum), Alain Froment, Philippe Mennecier and Aurelie Font (Musée de L'Homme, Paris), Chris Stringer and Rob Kruszynski (Natural History Museum, London), Jean-Jaques Cleyet-Merle (Musée National de Préhistoire, Les Eyzies de Tayac). Finally, they are also grateful to the two anonymous reviewers and the associated editor for their valuable comments and editing of the manuscript.

LITERATURE CITED

Akazawa T, Muhensen S, Dodo Y, Kondo O, Mizoguchi Y. 1995. Neanderthal infant burial. Nature 377:585–586.

Anderson DL, Thompson GW, Popovich F. 1976. Age of attainment of mineralization stages of the permanent dentition. J Forensic Sci 21:191–200.

Arsuaga JL, Bermúdez de Castro JM. 1984. Estudio de los restos humanos del yacimiento de la Cova del Tossal de la Font (Villafamés, Castellon). Cuadernos de Prehistoria y Arqueologia Castellonenses 10:19–34.

Arsuaga JL, Lorenzo C, Carretero JM, Gracia A, Martínez I, García N, Bermúdez de Castro JM, Carbonell E. 1999. A complete human pelvis from the Middle Pleistocene of Spain. Nature 399:255–258.

Arsuaga JL, Martínez I, Gracia A, Lorenzo C. 1997. The Sima de los Huesos crania (Sierra de Atapuerca, Spain): a comparative study. J Hum Evol 33:219–281.

Arsuaga JL, Villaverde V, Quam R, Martínez I, Carretero JM, Lorenzo C, Gracia A. 2007. New Neandertal remains from Cova Negra (Valencia, Spain). J Hum Evol 52:31–58.

Auerbach BM, Ruff CB. 2006. Limb bone bilateral asymmetry variability and commonality among modern humans. J Hum Evol 50:203–218.

Bacon AM. 2000. Principal components analysis of distal humeral shape in Pliocene to recent African hominids: the contribution of geometric morphometrics. Am J Phys Anthropol 111:479–487.

Basabe JM. 1966. El húmero premusteriense de Lezetxiki (Guipúzcoa). Munibe 1–4:13–32.

Berger GW, Pérez-González A, Carbonell E, Arsuaga JL, Bermúdez de Castro JM, Ku T-L. 2008. Luminescence chronology of cave sediments at the Atapuerca paleoanthropological site, Spain. J Hum Evol 55:300–311.

Bermúdez de Castro JM. 1993. The Atapuerca dental remains: new evidence (1987–1991 excavations) and interpretations. J Hum Evol 24:339–371.

Bermúdez de Castro JM, Arsuaga JL, Carbonell E, Rosas A, Martínez I, Mosquera M. 1997. A hominid from the Lower Pleistocene of Atapuerca, Spain: possible ancestor to Neandertals and modern humans. Science 276:1392–1395.

Bermúdez de Castro JM, Martinón-Torres M, Prado L, Gómez-Robles L, Rosell J, López-Polín L, Arsuaga JL, Carbonell E. 2010. New immature hominin fossil from European Lower Pleistocene shows the earliest evidence of a modern human dental development pattern. Proc Natl Acad Sci USA 26:11739–11744.

Bermúdez de Castro JM, Martinón-Torres M, Sarmiento S, Lozano M. 2003. Gran Dolina-TD6 versus Sima de los Huesos dental samples from Atapuerca: evidence of discontinuity in the European Pleistocene population? J Archaeol Sci 30:1421–1428.

Bermúdez de Castro JM, Pérez-González A, Martinón-Torres M, Gómez-Robles A, Rosell J, Prado L, Sarmiento S, Carbonell E. 2008. A new Early Pleistocene hominin mandible from Atapuerca-TD6, Spain. J Hum Evol 55:729–735.

Bermúdez de Castro JM, Rosas A, Nicolás ME. 1999. Dental remains from Atapuerca-TD6 (Gran Dolina site, Burgos, Spain). J Hum Evol 37:523–566.

Carbonell E, Bermúdez de Castro JM, Arsuaga JL, Allue E, Bastir M, Benito A, Cáceres I, Canals T, Díez JC, van der Made J, Mosquera M, Ollé A, Pérez-González A, Rodríguez J, Rodríguez XP, Rosas A, Rosell J, Sala R, Vallverdú J, Vergés JM. 2005. A new early Pleistocene hominin mandible from Atapuerca-TD6, Spain. Proc Natl Acad Sci USA 102:5674–5678.

Carbonell E, Bermúdez de Castro JM, Arsuaga JL, Díez JC, Rosas A, Cuenca-Bescós G, Sala R, Mosquera M, Rodriguez XP. 1995. Lower Pleistocene hominids and artifacts from Atapuerca-TD6 (Spain). Science 269:826–830.

Carbonell E, Cáceres I, Lozano M, Saladié P, Rosell J, Lorenzo C, Vallverdú J, Huguet R, Canals T, Bermúdez de Castro JM. 2010. Cultural cannibalism as a paleoeconomic system in the European Lower Pleistocene. Curr Anthropol 51:539–549.

Carbonell E, Esteban M, Martín-Nájera A, Mosquera M, Rodríguez XP, Ollé A, Sala R, Vergés JM, Bermúdez de Castro JM, Ortega AI. 1999. The Pleistocene site of Gran Dolina, Sierra de Atapuerca, Spain: a history of the archeological investigations. J Hum Evol 37:313–324.

Cardoso HFV. 2006. Brief communication: the collection of identified human skeletons housed at the Bocage museum (National Museum of Natural History), Lisbon, Portugal. Am J Phys Anthropol 129:173–176.

Carretero JM, Arsuaga JL, Lorenzo C. 1997. Clavicles, scapulae and humeri from the Sima de los Huesos site (Sierra de Atapuerca, Spain). J Hum Evol 33:357–408.

Carretero JM, Haile-Selassie Y, Rodríguez L, Arsuaga JL. 2009. A partial distal humerus from the Middle Pleistocene deposits at Bodo, Middle Awash, Ethiopia. Anthropol Sci 117:19–31.

Carretero JM, Lorenzo C, Arsuaga JL. 1999. Axial and appendicular skeleton of *Homo antecessor*. J Hum Evol 37:459–499.

Chavaillon J, Chavaillon N, Coppens Y, Senut B. 1977. Présence d'Hominidé dans le site oldowayen de Gomboré IB à Melka Kunturé, Ethiopie. CR Acad Sci Paris 285:961–963.

Churchill SE. 1994. Human upper body evolution in the Eurasian later Pleistocene. Albuquerque, NM: University of New Mexico.

Churchill SE, Pearson OM, Grine FE, Trinkaus E, Hollyday TW. 1996. Morphological affinities of the proximal ulna from Klasies River Main Site: archaic or modern? J Hum Evol 31:213–237.

Coqueugniot H, Weaver TD. 2007. Brief communication: infracranial maturation in the skeletal collection from Coimbra, Portugal: new aging standards for epiphyseal union. Am J Phys Anthropol 134:424–437.

Cowgill LW. 2010. The ontogeny of Holocene and Late Pleistocene human postcranial strength. Am J Phys Anthropol 141:16–37.

Cuenca-Bescós G, Laplana C, Canudo JI. 1999. Biochronological implications of the Arvicolidae (Rodentia, Mammalia) from the Lower Pleistocene hominid-bearing level of Trinchera Dolina 6 (TD6, Atapuerca, Spain). J Hum Evol 37:353–373.

Day M, Twist M, Ward S. 1991. Les vestiges post-craniens d'Omo 1 (Kibish). L'Anthropologie 95:595–610.

Dodo Y, Kondo O, Muhensen S, Akazawa T. 1998. Anatomy of the Neandertal infant skeleton from Dederiyeh Cave, Syria. In: Akazawa T, Aoki K, Bar-Yosef O, editors. Neandertals and modern humans in Western Asia. New York: Plenum. p 323–338.

Endicott P, Ho SYW, Stringer C. 2010. Using evidence to evaluate four paleoanthropological hypotheses for the timing of Neanderthal and modern human origins. J Hum Evol 59:87–95.

Falguères C, Bahain J-J, Yokoyama Y, Arsuaga JL, Bermúdez de Castro JM, Carbonell E, Bischoff JL, Dolo JM. 1999. Earliest humans in Europe: the age of TD6 Gran Dolina, Atapuerca, Spain. J Hum Evol 37:343–352.

Fazekas GI, Kosa F. 1978. Forensic foetal osteology. Budapest: Akademiai Kiado.

Fernández-Jalvo Y, Díez JC, Bermúdez de Castro JM, Carbonell E, Arsuaga JL. 1996. Evidence of early cannibalism. Science 271:277–278.

Fernández-Jalvo Y, Díez JC, Cáceres I, Rosell J. 1999. Human cannibalism in the Early Pleistocene of Europe (Gran Dolina, Sierra de Atapuerca, Burgos, Spain). J Hum Evol 37:591–622.

Gabunia L, Vekua A, Lordkipanidze D, Swisher ICC III, Ferring R, Justus A, Niorazde M, Tvalcrelidze M, Anton S, Bosinski G, Jöris O, Lumley MA de, Majsuradze G, Mouskhelisvili A. 2000. Earliest Pleistocene hominid cranial remains from Dmanisi, Republic of Georgia: taxonomy, geological setting, and age. Science 288:1019–1025.

García N, Arsuaga JL. 1999. Carnivores from the Early Pleistocene hominid-bearing Trinchera Dolina 6 (Sierra de Atapuerca, Spain). J Hum Evol 37:415–430.

García-Antón M. 1995. Pollen analysis of Middle Pleistocene paleovegetation at Atapuerca. In: Bermúdez de Castro JM, Arsuaga JL, Carbonell E, editors. Human evolution in Europe and the Atapuerca evidence. Valladolid: Junta de Castilla y León. p 147–165.

García-González R, Carretero JM, Rodríguez L, Gómez A, Arsuaga JL, Bermúdez de Castro JM, Carbonell E, Martínez I, Lorenzo C. 2009. Étude analytique d'une clavicule complète de subaulte d'*Homo antecessor* (site de Gran Dolina, Sierra d'Atapuerca, Burgos, Espagne). L'Anthropologie 113:222–232.

Gómez Olivenza A, Carretero JM, Lorenzo C, Arsuaga JL, Bermúdez de Castro JM, Carbonell E. 2010. The costal skeleton of *Homo antecessor*: first results. J Hum Evol 59:620–640.

Gómez-Robles A, Martinón-Torres M, Bermúdez de Castro JM, Margvelashvili A, Bastir M, Arsuaga JL, Pérez-Pérez A, Estebaranz F, Martínez LM. 2007. A geometric morphometric analysis of hominin upper first molar shape. J Hum Evol 53:272–285.

Green RE, Malaspinas A-S, Krause J, Briggs AW, Johnson PLF, Uhler C, Meyer M, Good JM, Maricic T, Stencel U, Prüfer K, Siebauer M, Burbano HA, Ronan M, Rothberg JM, Egholm M, Rudan P, Brajkovic D, Kucan Z, Gusic I, Wikström M, Laakkonen L, Kelso J, Slatkin M, Pääbo S. 2008. A complete Neandertal mitochondrial genome sequence determined by high-throughput sequencing. Cell 134:416–426.

Groves CP. 1998. The proximal ulna from Klasies River. J Hum Evol 34:119–121.

Heim JL. 1982. Les homes fossils de la Ferrasie. Tome II. Les squelettes adultes (squelettes des members). Arch Inst Pal Hum 38:1–272.

Johanson DC, Masao FT, Eck GG, White TD, Walter RC, Kimbel WH, Asfaw B, Manega P, Ndessokiam P, Suwa G. 1987. New partial skeleton of *Homo habilis* from Olduvai Gorge, Tanzania. Nature 327:205–209.

Kondo O, Dodo Y. 2002. The postcranial bones of the Neanderthal child of burial N°1. In: Akazawa T, Muhesen S, editors. Neanderthal burials. Excavations of the Dederiyeh Cave, Afrin, Syria. Kyoto: International Research Center for Japanese Studies. p 139–214.

Kondo O, Dodo Y, Akazawa T, Muhesen S. 2000. Estimation of stature from the skeletal reconstruction of an immature Neandertal from Dederiyeh Cave, Syria. J Hum Evol 38: 457–473.

Krause J, Fu Q, Good JM, Viola B, Shunkov MV, Derevianko AP, Pääbo S. 2010. The complete mitochondrial DNA genome of an unknown hominin from southern Siberia. Nature 464:894–897.

Lague MR, Jungers WL. 1996. Morphometric variation in Plio-Pleistocene hominid distal humeri. Am J Phys Anthropol 101:401–427.

Larson SG, Jungers WL, Morwood MJ, Sutikna T, Wahyu Saptomo JE, Due RA, Djunoantono T. 2007. *Homo floresiensis* and the evolution of the hominin shoulder. J Hum Evol 53:718–731.

Lorenzo C, Arsuaga JL, Carretero JM. 1999. Hand and foot remains from the Gran Dolina Early Pleistocene site (Sierra de Atapuerca, Spain). J Hum Evol 37:501–522.

Lordkipanidze D, Jashashvili T, Vekua A, Ponce de León M, Zollikofer CPE, Rightmire GP, Pontzer H, Ferring R, Oms O, Tappen M, Bukhsianidze M, Agustí J, Kahlke R, Liladze G, Martínez-Navarro B, Mouskhelisvili A, Nioradze M, Rook L. 2007. Postcranial evidence from early *Homo* from Dmanisi, Georgia. Nature 449:305–310.

Lumley H de, Lordkipanidze D, Féraud G, Garcia T, Perrenoud C, Falguères C, Gagnepain J, Saos T, Voinchet P. 2002. Datation par la méthode $^{40}Ar/^{39}Ar$ de la couche de cendres volcaniques (couche VI) de Dmanissi (Géorgie) qui a livré des restes d'hominidés fossiles de 1,81 Ma. Palevol 1:181–189.

Made J van der. 1999. Ungulates from Atapuerca-TD6. J Hum Evol 37:389–413.

Madre-Dupouy M. 1992. L'enfant du Roc de Marsal. Étude analytique et comparative. Cahiers de Paléoanthropologie. Éditions du CNRS.

Maresh MM. 1970. Measurements from roentgenograms. In: McCammon RW, editor. Human growth and development. Springfield, IL: C.C. Thomas. p 157–200.

Martinón-Torres M, Bastir M, Bermúdez de Castro JM, Gómez-Robles A, Sarmiento S, Muela A, Arsuaga JL. 2006. Hominin lower second premolar morphology: evolutionary inferences through geometric morphometrics analysis. J Hum Evol 50:523–533.

Martinón-Torres M, Bermúdez de Castro JM, Gómez-Robles A, Arsuaga JL, Carbonell E, Lordkipanidze D, Manzi G, Margvelashvili A. 2007. Dental evidence on the hominin dispersals during the Pleistocene. Proc Natl Acad Sci USA 104:13279–13282.

Martinón-Torres M, Bermúdez de Castro JM, Gómez-Robles A, Prado-Simón L, Arsuaga JL. Morphological description and comparison of the dental remains from Atapuerca-Sima de los Huesos site (Spain). J Hum Evol 62:7–58.

McCown TD, Keith A. 1939. The stone age of Mount Carmel II: the fossil human remains from the Levallois-Mousterian. Oxford: Clarendon Press.

McHenry HM, Corruccini RS. 1975. Distal humerus in hominoid evolution. Folia Primatologica 23:227–244.

Minugh-Purvis N. 1988. Patterns of craniofacial growth and development in Upper Pleistocene hominids. Ph.D. Dissertation, University of Pennsylvania.

Moorrees CFA, Fanning EA, Hunt EE. 1963a. Age variation of formation stages for ten permanent teeth. J Dent Res 42:1490–1502.

Moorrees CFA, Fanning EA, Hunt EE. 1963b. Formation and resorption of three deciduous teeth in children. Am J Phys Anthropol 21:205–213.

Noonan JP, Coop G, Kudaravalli S, Smith D, Krause J, Chen JAF, Platt D, Pääbo S, Pritchard JK, Rubin EM. 2006. Sequencing and analysis of Neanderthal genomic DNA. Science 314:1113–1118.

Ovchinnikov IV, Götherström A, Romanova GP, Kharitonov GP, Lidén K, Goodwin W. 2002. Molecular analysis of Neandertal DNA from the northern Caucasus. Nature 404:490–493.

Parés JM, Pérez-González A. 1995. Paleomagnetic age for hominid fossils at Atapuerca archeological site, Spain. Science 269:830–832.

Parés JM, Pérez-González A. 1999. Magnetochronology and stratigraphy at Gran Dolina section, Atapuerca (Burgos, Spain). J Hum Evol 37:325–342.

Pearson OM. 1999. Postcranial differences between the earliest modern humans and recent people. J Hum Evol 36:A16–A17.

Pearson OM, Churchill SE, Grine FE, Trinkaus E, Holliday TW. 1998. Multivariate analyses of hominid ulna from Klasies River Mouth. J Hum Evol 34:653–656.

Pearson OM, Grine FE. 1996. Morphology of the Border Cave hominid ulna and humerus. S Afr J Sci 92:231–236.

Pfeiffer S, Zehr MK. 1996. A morphological and histological study of the human humerus from Border Cave. J Hum Evol 31:49–59.

Pycraft WP, Smith GE, Yearsley M, Carter JT, Smith RA, Hopwood AT, Bate DMA, Swinton WE. 1928. Rhodesian man and associated remains. London: The British Museum, Natural History.

Roberts GJ, Parekh A, Petrie A, Lucas VS. 2008 Dental age assessment (DAA): a simple method for children and emerging adults. Br Dent J 204:E7.

Rosas A, Bermúdez de Castro JM. 1999. The ATD6-5 mandibular specimen from Gran Dolina (Atapuerca, Spain). Morphological study and phylogenetic implications. J Hum Evol 37:567–590.

Rosenberger KR, Zuné L, Ruff CB. 2006. Body size, body proportions and encephalization in a Middle Pleistocene archaic human from northern China. Proc Natl Acad Sci USA 103:3552–3556.

Ruff CB. 2008. Femoral/humeral strength in early African *Homo erectus*. J Hum Evol 54:383–390.

Ruff CB. 2009. Relative limb strength and locomotion in *Homo habilis*. Am J Phys Anthropol 138:90–100.

Ruff CB, Hayes WC. 1983. Cross-sectional geometry of Pecos Pueblo femora and tibiae: a biomechanical investigation: I. Method and general patterns of variation. Am J Phys Anthropol 60:359–381.

Ruff CB, Trinkaus E, Walker A, Larsen, C. 1993. Postcranial Robusticity in *Homo* I: temporal trends and mechanical interpretation. Am J Phys Anthropol 91:21–53.

Ruff CB, Walker A, Trinkaus E. 1994. Postcranial robusticity in *Homo*. III: ontogeny. Am J Phys Anthropol 93:35–54.

Shang H, Tong H, Zhang S, Chen F, Trinkaus E. 2007. An early modern human from Tianyuan Cave, China. Proc Natl Acad Sci USA 104:6573–6578.

Shang H, Trinkaus E. 2010. The early modern human from Tianyuan Cave, China. College Station, TX: Texas A&M University Press.

Sládek V, Trinkaus E, Hillson SW, Holliday T. 2000. Skeletal catalogue and osteometrics of the Gravettian fossil hominids from Dolní Vestonice and Pavlov. Brno: Academy of Science of the Czech Republic, Institute of Archeology.

Scheuer L, Black S. 2000. Developmental juvenile osteology. Oxford: Elsevier Academic Press.

Scheuer L, Musgrave JH, Evans SP. 1980. The estimation of late fetal and perinatal age from limb bone length by linear and logarithmic regression. Ann Hum Biol 7:257–265.

Senut B. 1981. Humeral outlines in some hominoid primates and in Plio-Pleistocene hominids. Am J Phys Anthropol 56:275–283.

Smith SL, Buschang PH. 2004. Variation in longitudinal diaphyseal long bone growth in children three to ten years of age. Am J Hum Biol 16:648–657.

StatSoft, Inc. 2001. STATISTICA (data analysis software system), version 6. Available at:www.statsoft.com.

Themido AA. 1926. Sôbre alguns caracteres sexuais dos húmeros portugueses. Revista da Universidade de Coimbra. 10:104–173.

Tillier AM. 1999. Les Enfants Moustériens de Qafzeh. Interprétation phylogénétique et paléoauxologique. Paris: CNRS edn.

Trinkaus E, Churchill SE. 1999. Diaphyseal cross-sectional geometry of Near Eastern Middle Paleolithic humans: the humerus. J Archaeol Sci 26:173–184.

Trinkaus E, Churchill SE, Ruff CB. 1994. Postcranial robusticity in *Homo*. II: humeral asymmetry and bone plasticity. Am J Phys Anthropol 93:1–43.

Trinkaus E, Churchill SE, Ruff CB, Vandermeersch B. 1999. Long bone shaft robusticity and body proportions of Saint-Cesaire 1 Chatelperronian Neanderthal. J Archaeol Sci 26:755–773.

Trinkaus E, Ruff C, Esteves F, Santos-Coelho J, Silva M, Mendonca M. 2002. The upper limb remains. In: Zilhao J, Trinkaus E, editors. Portrait of the artist as a child: the Gravettian human skeleton from the Abrigo do Lagar Velho and its archeological context . Trabalhos de Arqueologia22:466–488.

Trinkaus E, Svoboda J, editors. 2006. Early modern human evolution in Central Europe. Oxford: Oxford University Press.

Villa P, Mahieu E. 1991. Breakage patterns of human long bones. J Hum Evol 21:27–48.

Vlcêk E. 1973. Postcranial skeleton of a Neandertal child from KiiK-Koba, USSR. J Hum Evol 2:537–544.

Wainright SA, Biggs WD, Currey JD, Gosline JM. 1976. Mechanical design in organisms. Princeton, NJ: Princeton University Press.

Walker A, Leakey REF. 1993. The Nariokotome *Homo erectus* skeleton. Berlin: Springer Verlag.

Yokley TR, Churchill SE. 2006. Archaic and modern human distal humeral morphology. J Hum Evol 51:603–616.

Zilhao J, Trinkaus E, editors. 2002. Portrait of the artist as a child: the Gravettian human skeleton from the Abrigo do Lagar Velho and its archeological context. Lisboa: Instituto Portugues de Arqueologia.